RESEARCH ARTICLE

Mechanical and Structural Properties of $Zn_{0.1}Ni_{0.4}Cu_{0.5}Fe_2O_4$ Ferrite

Shridhar N. Mathad
Department of Physics, KLEIT, Gokul, Hubballi-580030, India

ABSTRACT: Polycrystalline Zn-Ni-Cu ferrite with general formula $Zn_{0.1}Ni_{0.4}Cu_{0.5}Fe_2O_4$ ferrite has been prepared by solid state method. In order to explore the structural parameters of prepared samples were characterized by using X-ray diffraction (XRD), Fourier Transform Infrared Spectroscopy (FT-IR) technique. The lattice parameter was found to 8.463A^0. Texture coefficient (TC) of (422) is 2.1212.The orientation grain growth is more in (422) plain. The FT-IR spectra of spinel ferrite and has attributed the band around 600 cm^{-1} to the intrinsic vibrations of tetrahedral complexes corresponding to the highest restoring force and the band around 400 cm^{-1} to intrinsic vibrations of octahedral complexes. Crystallite size (D), interatomic bond-lengths, hopping lengths, train and dislocation density (ρ_D) also reported.

KEYWORDS: Ferrites, XRD, FT-IR and texture analysis.

https://doi.org/10.29294/IJASE.5.2.2018.911-916

1. INTRODUCTION

Ferrites are beneficial dielectric materials with low conductivity and which have wide applications in the field of micro-wave devices [1,2]. Ferrites are technologically significant materials because of their unparalleled electric, dielectric, magnetic and optical properties, which makes them suitable for many technological applications like microwave devices, transformers, electric generators, storage devices etc [3]. Multilayer chip inductors [MLCIs] and microspiral inductors developed by thick film printing and co-firing technologies using low temperature-sintered Ni-Cu-Zn ferrite and Ag. Ni-Cu-Zn ferrites have been developed to meet a demand for miniaturization of electronic components [3-5]. Nickel ferrite is an inverse spinal magnetic ferrite, while to that Zinc ferrite is normal spinel structure. The Ni-Zn mixed spinel ferrites have attracted research activities due to high resistivity, high permeability, low loss and high Curie temperature [1,7]. The substituted nickel ferrites are extensive examine scientifically because of unique microwave applications such as circulators, isolators, phase shifters, etc., due to its low electrical conductivity, squareness of hysteresis loop [8].Electrical and magnetic properties of ferrites are highly reliant on cation distribution, which in turn controlled by preparation methodology, composition and nature of impurity ions present in the material. Ferrites are synthesized by several methods like ceramic method [9], sol-gel Method [10], microwave method [11], combustion method [11], thermal treatment method, sucrose method [12], EDTA-assisted hydrothermal method [13], micro-emulsion and thermolysis [14], oxalate co-precipitation technique [15].

The main aim of this paper is to synthesize the $Zn_{0.1}Ni_{0.4}Cu_{0.5}Fe_2O_4$ ferrite by solid state reaction. X-ray diffraction (XRD) was used understand the cubic phase and Fourier Transform Infrared Spectroscopy (FT-IR) technique was employed to empathize the finger print vibrations of ferrites. We have investigated the fundamental structural parameters like crystallite size (D), Texture analysis, interatomic bond-lengths, hopping lengths and dislocation density (ρ_D) of ferrite.

2. Experimental method

Using Solid-state method was employed to prepare the ferrites with the general formula $Zn_{0.1}Ni_{0.4}Cu_{0.5}Fe_2O_4$ ferrite. High purity oxides of nickel, zinc, copper and iron were weighed accurately by using a microbalance in the required molar proportions and mixed mechanically in agate mortar in acetone medium. All samples were pre-sintered at 800^0C for 10 hours and final sintering at 1100^0C furnace for 15 hours to enable complete solid state reaction. After that the fine powders were once again milled in agate mortar for 2-3 hrs and mixed with 2-3 drops of polyvinyl alcohol as a binder. The constituent powders were pressed into pellets of 10-15 mm diameter and 2-4 mm thickness using a hydraulic press by applying a pressure of about 7 tones/$inch^2$ for 6-7 minutes. The pellets were finally sintered at 900ºC for 4 hrs in a muffle furnace and then cooled to room temperature in air to yield the end product. The samples were furnace cooled in air medium. The schematic flow of the work is shown in Fig.1.

3. Results and Discussions

3.1 Structural studies

Fig. 2 shows the $Zn_{0.1}Ni_{0.4}Cu_{0.5}Fe_2O_4$ X-ray diffraction patterns for the composition. The main reflection planes of the spinel structure of ferrites are shown in the X-ray patterns where these planes are (111), (220), (311), (222), (400), (511) and (440). All planes in XRD chart

**Corresponding Author: physicssiddu@gmail.com*
Received: 17.09.2018 **Accepted:** 18.10.2018 **Published on**: 27.11.2018

were compared and indexed using ICDD card no. 49-0266. Detailed analysis of lattice parameter was tabulated in Table 1. Average Cryatallite size is calculated by Debye-Scherrer's formula [17]

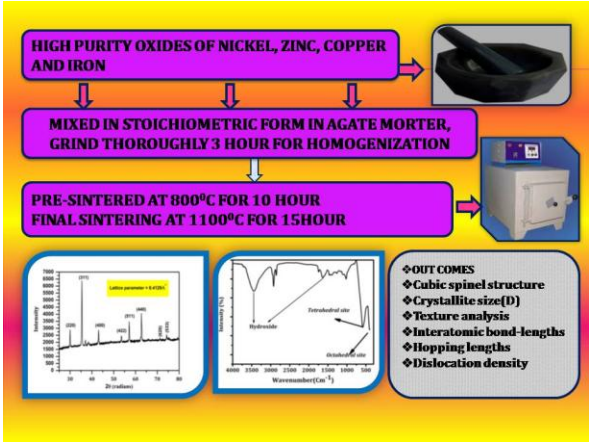

Fig.1 Schematic flow chart of ferrite sample

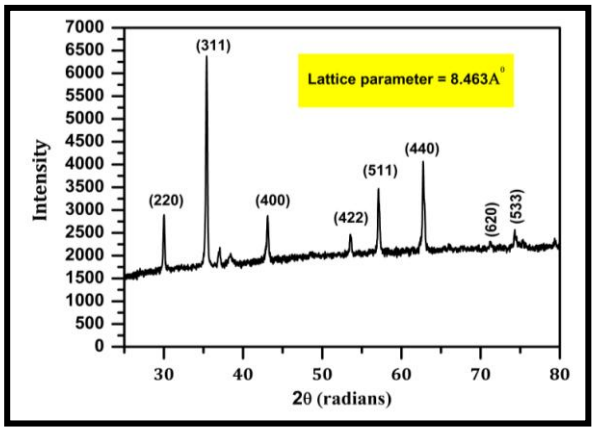

Fig.2 X-ray diffraction pattern of Ferrite sample

$$D = \frac{K \cdot \lambda}{\beta_D . \cos\theta} \quad (1)$$

Where, D- Crystallite size, λ- wavelength of x-ray used (1.5406 Å), K- Crystallite shape factor which is taken as 0.9 in this case considering the particles to be spherical in general. β_D- pure diffraction broadening.

$$(\Delta x_{Ferrite}) = \frac{8M}{Na^3} \quad (2)$$

Where, $\Delta x_{ferrite}$-x-ray density, M- molecular weight of sample, N- Avogadro's number

$$L_A = \frac{a \times \sqrt{3}}{4} \quad (3)$$

$$L_B = \frac{a \times \sqrt{2}}{4} \quad (4)$$

Where, L_A-The distance between magnetic ions (hopping length) in A site (Tetrahedral) and L_B-B site (Octahedral).

$$A - O = (u - 1/4)a\sqrt{3} \quad (5)$$

$$B - O = (5/8 - u)a \quad (6)$$

Where, A-O – bond length between A ion and Oxygen, B-O – bond length between A ion and Oxygen, u-oxygen ion parameter [17]

$$r_A = (u - 1/4)a\sqrt{3} - r(O^{2-}) \quad (7)$$

$$r_B = (5/8 - u)a - r(O^{2-}) \quad (8)$$

Where, r_A– ionic radii for A site, r_B– ionic radii for B site, $r(O^{2-})$- ionic radii of Oxygen ion (1.35Å).

All the structural parameters like lattice parameter, crystallite size, hopping length and density was tabulated in Table No.2

3.2 Mechanical properties

Lattice micro strain (ε) is a term used more oftenly in material engineering. Strain is defined as the deformation of an object divided by it is the ideal length. Dislocations are one-dimensional crystalline defects marking the boundary between a slipped and an unslipped region of a material. This defect distorts the regular atomic array of a perfect crystal. The amount of the defects in the as deposited film was resolved by evaluating the dislocation density. The dislocation density (ρ_D) is a measure of the number of dislocations in a unit volume of a crystalline material. The smaller the value of dislocation densities and larger grains is the indication of the better crystallization.

$$micro - strain(\varepsilon) = \frac{\beta \cos\theta}{4} \quad (9)$$

$$\text{Dislocation Density } (\rho_D) = \frac{1}{D^2} \quad (10)$$

$$\rho_D = \frac{15\varepsilon}{aD} \quad (11)$$

The crystallite size, micro-strain and dislocation density are tabulated in Table.3.

3.3 Texture analysis

The preferred orientation of crystallites may result from the nature of the material, which is pronounced on the physical and mechanical properties of material. The reflection intensities from each XRD pattern contain information related to the preferential growth of polycrystalline ferrite was studied by calculating the texture coefficient TC (hkl) for high level orientation. Quantitative information concerning the preferential crystallite orientation is obtained from texture

coefficient. TCs (hkl) were calculated by using the relation [18].

$$TC(hkl) = \frac{\frac{I(hkl)}{I_0(hkl)}}{\frac{1}{N}\sum_N \frac{I(hkl)}{I_0(hkl)}} \quad (12)$$

Where I (hkl) is the measured intensity, I_0 (hkl) is the ASTM intensity and N the reflection number. The calculated texture coefficient (TC) of each plane (hkl) is tabulated in Table 4. Texture coefficient (TC) of (422) is 2.1212.The orientation grain growth is more in (422) plain.

3.4 Williamson Hall plot and Size-Strain Plot Method

The size and strain broadening of peaks are additive components of the total integral breadth of a Bragg peak [19]. The distinct θ dependencies of both effects laid the basis for the separation of size and strain broadening in the analysis of Williamson and Hall. The W-H plot is plotted using Eq.13 are plotted in Fig.3

$$\beta_{hkl}\cos\theta = \frac{K\cdot\lambda}{D} + 4\varepsilon\sin\theta \quad ...(13)$$

The evaluation of the size-strain parameters are obtained by considering peaks in average range, which has the advantage that less weight is given to data from reflections at high angles, where the precision is usually less, the SSP plots are shown in Fig.4 which are plotted using Eq.(14). In this approximation, SSP plots assume that the ''crystallite size'' profile is Lorentzian and the ''strain profile'' by a Gaussian function [20,21]
Accordingly, we have:

$$(d_{hkl}\beta_{hkl}\cos\theta)^2 = \frac{K.\lambda}{D}(d_{hkl}^2\beta_{hkl}\cos\theta) + \left(\frac{\varepsilon}{2}\right)^2 \quad ... (14)$$

All mechanical properties are in good agreement with both method and also with equation 9,10 and 11. The correlation between W-H plot and SSP has been reported in Table.3.

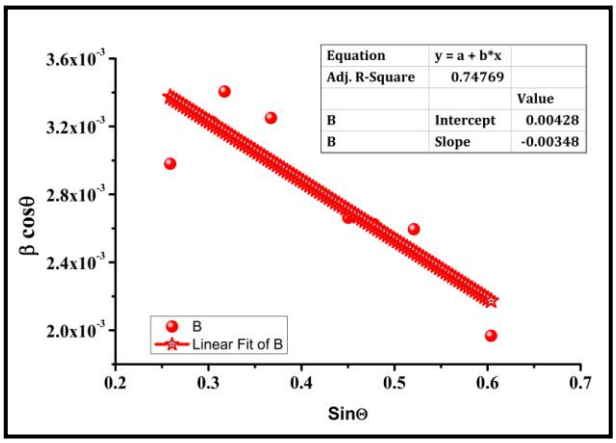

Fig.3 Plot of βcosθ versus sinθ (Williamson-Hall plot)

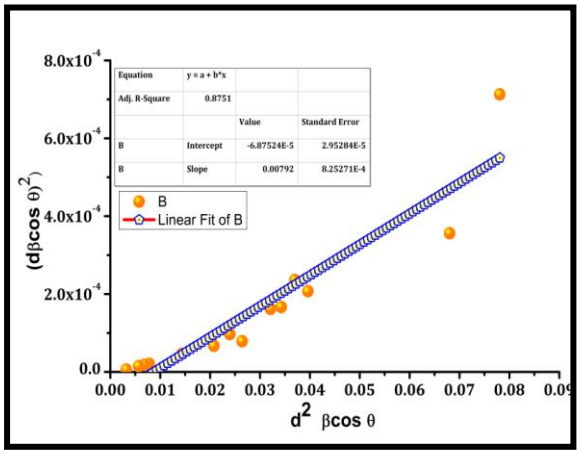

Fig. 4 Size-Strain Plot of ferrite sample

Table.1 Lattice parameter

Sl. No.	Angle 2θ	SinΘ	Calculated d (Å)	Miller indices			Lattice parameter a (Å)
				h	k	l	
1	29.94	0.2582	2.980	2	2	0	8.4287
2	35.32	0.3033	2.5413	3	1	1	8.4285
3	36.97	0.3170	2.4331	2	2	2	8.4285
4	43.00	0.3664	2.1071	4	0	0	8.4284
5	53.42	0.4494	1.7205	4	2	2	8.4287
6	56.97	0.4768	1.622	5	1	1	8.4282
7	62.59	0.5194	1.490	4	4	0	8.4287
8	71.08	0.5812	1.3327	5	3	3	8.7391
9	74.14	0.6027	1.2706	6	2	2	8.4282
					Lattice parameter		*8.4630*

3.5 FT-IR studies of ferrites

The spinel ferrites crystallize in the cubic spinel form with space group Fd_{3m}-O^7_h [9,22].On the basis of group theoretical calculations, it has been demonstrated that the spinel ferrites exhibit four IR active fundamentals in the vibrational spectra of normal as well as inverse spinel ferrites. It has been reported that first three IR bands are due to the tetrahedral (T_d) and octahedral (O_h) coordination compounds, while the fourth one is due some type of lattice vibrations involved with tetrahedral cations [22]. The IR absorption spectra of the ferrite sample as shown in the Fig.5. According to Waldon [23] the IR spectra of spinel ferrites and has attributed the band ν_1 around 600 cm^{-1} to the intrinsic vibrations of tetrahedral complexes corresponding to the highest restoring force and the band ν_2 around 400 cm^{-1} to intrinsic vibrations of octahedral complexes. Therefore it is expected that $\nu_1 > \nu_2$. Both ν_1 and ν_2 bands depend on the nature of octahedral cations significantly but not on the nature of octahedral ions. The ν_1 is found at 565 cm^{-1} and ν_2 is found at 405 cm^{-1}. The difference in the band positions is attributed to the difference in the Fe^{3+}-O^{2-} distance for the octahedral and tetrahedral coordination compounds. Waldron *et.al* [23] had attributed that the occurrence of ν_1 and ν_2 bands to the intrinsic vibrations of the tetrahedral **[T_d]** and octahedral **[O_h]** coordination compounds.

The inter-atomic distances like tetrahedral bond length (d_{Ax}), Octahedral bond length(d_{Bx}), Shared tetragonal edge (d_{AEx}), Shared octahedral edge(d_{BxE}) and unshared octahedral edge(d_{BxEu}) has been calculated [9,24]

$$d_{Ax} = a(u - 1/4)\sqrt{3} \quad --(15)$$

$$d_{Bx} = a[3u^2 - \frac{11}{4}u + \frac{43}{64}]^{1/2} \quad --(16)$$

$$d_{AEx} = a(2u - \frac{1}{2})\sqrt{2} \quad --(17)$$

$$d_{BxE} = a(1 - 2u)\sqrt{2} \quad --(18)$$

$$d_{BxEu} = a\sqrt{[4u^2 - 3u + \frac{11}{16}]} \quad --(19)$$

The interionic distances between the cations (Me-Me) (b, c, d, e, and f) and between the cation and anion (Me-O) (p, q, r and s) were calculated as described in our previous papers [9]. In the A-A and B-B cases, the angles are too small or the distances between the metal ions (M_e) and the oxygen ions (O) are too large. The best combinations of distances and angles are found in the A-B interactions. Thus all the interatomic distance (Me-Me) and the cation and anion (Me-O) tabulated in Table 6.

Table.2 Lattice parameter, volume, hopping lengths and bond lengths

Lattice parameter a (Å)	Volume of unit cell V (10^{-30})	Hopping length L_A (Å)	Hopping length L_B (Å)	Bond Length A-O (Å)	Bond length A-B (Å)	Ionic Radii r_A (Å)	Ionic Radii r_B (Å)
8.4630	606.14	3.6646	2.9921	1.8323	2.1158	0.4823	0.7658

Table.3 Crystallite size, micro-strain and dislocation density

Crystallite size (in nm)			Micro strain			Dislocation density (σ)	
From W-H graph	From SSP	From formula	Micro strain ε=slope/4 (WH)	Micro strain ε=2*sqrt(slope) (SSP)	From formula ε=βcosθ/4	$\sigma=1/D^2$	$\sigma=15\varepsilon/aD$
21	35	44	0.00198	0.00258	0.00226	$5.165X10^{14}$	$9X10^{14}$

Table.5 Edge length and bond lengths

Lattice parameter	Edge and bond lengths (A°)				
a	d_{Ax}	d_{Bx}	d_{AxE}	d_{BxE}	d_{BxEu}
8.4652	0.152486	1.160886	0.249009	5.736791	3.56678

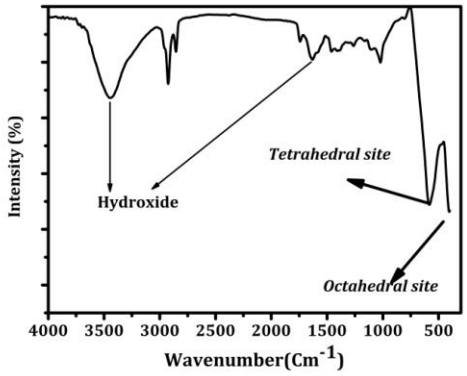

Fig.5 FT-IR spectra of ferrite

Table.4 Texture analysis of Ferrite sample

Miller indices (hkl)			Texture analysis
h	k	l	TC (hkl)
1	1	1	0.2587
2	2	0	0.5928
3	1	1	0.6467
2	2	2	0.3245
4	0	0	0.6758
4	2	2	2.1212
5	1	1	0.7437
4	4	0	1.0557
6	2	0	1.1317
5	3	3	1.0275
4	4	4	1.7461

Table No.6 Me-Me and Me-O bond lengths

Me–Me distance (A°)					Me–O distance (A°)				Vibrational bands (cm-1)	
b	c	d	e	f	p	q	r	s	ν_1	ν_2
2.9914	3.5078	3.6637	5.4956	5.1813	1.9884	2.0517	3.9288	3.7370	405	565

4. CONCLUSION

In this paper, we have used XRD and FT-IR spectra to explore the structural studies of Zn-Ni-Cu ferrite. XRD confirms the cubic system with lattice parameter with 8.463A°. Absorption bands of spinel ferrite have appeared through IR absorption spectra recorded in the range of 400–600 cm^{-1} and interpreted in terms of binding forces. The orientation grain growth is more in (422) plain. All mechanical properties are in good agreement with SSP and WH plots.

REFERENCES

[1] Goldman, A. 2006. Modern Ferrite Technology, second ed., Springer, New York, 2006.

[2] Harris, V.G., 2012. Advances in magnetics: Modern microwave ferrites, IEEE Trans. Magn .,48(3), 1075–1105.

[3] Gubbala, S., H. Nathani, K. Koziol and R. D. K. Misra,2004. "Magnetic Properties of Nanocrystalline Ni-Zn, Zn-Mn, and Ni-Mn Ferrites Synthesized by Reverse Micelle Technique," Physica B: Condensed Matter, 348(1-4), 317-328.

[4] Fujimoto M.,1994. Inner stress induced by Cu metal precipitation at grain boundaries in low-temperature-fired Ni-Zn-Cu ferrite. J Am Ceram Soc, 77, 2873-2878.

[5] Batoo and Ansari, 2012. Low temperature-fired Ni-Cu-Zn ferrite nanoparticles through auto combustion method for multilayerchip inductor applications. Nanoscale Research Letters, 7:112.

[6] Akther. M. N., Yahya, N., Hussain, P. B.,2009. Structural and magnetic characterizations of nano structured Ni0. 8Zn0. 2Fe2O4 prepared by self combustion method, Int. J. Basic and Appl.Sci. 9 151

[7] Reynolds. T.G.,1988. Ferrites magnetic ceramic in: R.C.Buchanan (Ed.) Ceram. mater .Electron. Marcel Dekker, Inc.Ny.

[8] Sugimoto, M., 1999. The past, present, and future of ferrites, Journal of the American Ceramic Society, - Wiley Online Library

[9] Patil, M.R., Rendale, M.K., Mathad, S. N., and Pujar, R.B.,2015. "Structural and IR study of $Ni_{0.5-x}Cd_xZn_{0.5}Fe_2O_4$",International Journal of Self-Propagating High Temperature Synthesis, , Vol. 24, No. 4, pp. 241–245,

[10] Chae, K.P., Choi, W.O., Lee, J.C., Kang, B.S., Choi. S.H.,2013. J.Mag. 18 No 1, 21

[11] Molakeri, A. S., Kalyane,S., Mathad, S.N.,2017. Elastic Properties of nickel ferrite synthesized by combustion and microwave method using FT-IR spectra, International Journal of Advanced Science and Engineering, 3 (4) 422-427.

[12] Rendale, M.K., Mathad, S.N., Puri, V., 2015, Thick films of magnesium zinc ferrite with lithium substitution: Structural characteristics, Int. J.

Self-Propag. High- Temp. Synth, 24(2), pp.78–84

[13] Sachin V. Bangale, S. R. Bamane,2011. "Synthesis characterization and electrical properties of nanocrystallineZnMgO by combustion route" Der Chemica Sinica, 2(5),22-29

[14] Bao, N.Z., Shen, L.M., Wang, Y.H., Padhan,P., Gupta,A.,2007."A Facile Thermolysis Route to Monodisperse Ferrite Nanocrystals", J. Am. Chem. Soc., 129(41), 12374–12375

[15] Shedam, R.M., Gadkari, A. B., Mathad, S. N., Shedam , M. R.,2016 "Synthesis and structural investigation of nano-sized cadmium ferrite". Journal of Modern Materials, 2 (1), 7-12,

[16] Mathad, S. N., Puri. V.2012. "Structural and dielectric properties of $Sr_xBa_{1-x}Nb_2O_6$ ferroelectric ceramics" Archives of Physics Research, 3(2), 106-115

[17] Pathan, A.T, Mathad, S.N., Shaikh, A. M.,2014. "Infrared Spectral studies of Co^{2+} substituted Li-Ni-Zn Nano-structured Ferrites", International Journal of Self-Propagating High Temperature Synthesis, 23(2), 112–117.

[18] Mathad, S.N., Jadhav, R.N., Phadtare, V., Puri, V.,2014. "Structural and Mechanical Properties of Strotium doped Barium Niobate Thick-films", International Journal of Self-Propagating High Temperature Synthesis, 23(3).

[19] Khorsand Z. A., Ebrahimizadeh A.M., Abd. Majid, W.H., Ramin Yousefi, Hosseini, S.M.,2011. X-ray analysis of ZnO nanoparticles by WilliamsoneHall and sizeestrain plot methods, Ceram. Inter. 37, 393-398.

[20] Yendrapati,T.P., Kalagadda,V. R, Vemula S. S. K., Bandla Siva Kumari , 2014. X-Ray Analysis by Williamson-Hall and Size-Strain Plot Methods of ZnO Nanoparticles with Fuel Variation, World Journal of Nano Science and Engineering, 4, 21-28

[21] Kulkarni, A. B., Mathad, S.N.,2018. Synthesis and structural analysis of Co-Zn-Cd ferrite by Williamson-Hall and Size-Strain Plot Methods, International Journal of Self-Propagating High-Temperature Synthesis, 27, (1), 37–43.

[22] Kakatkar, S.V., Sankpal,A.M., Sawant, S.R., Suryavanshi, S.S., Ghodake, U.R, Kamat, R.K.,1994 Infrared absorption of Ti^{4+} and Zr^{4+} substituted Li-Zn ferrites, Indian journal of pure & applied physics,2, 193-194

[23] Waldron R. D.,1953 Infrared Spectra of Ferrites, Phys. Rev., 99 1727

[24] Lakhani, V. K., Pathak, T. K., Vasoya, N. H., Modi,K.B.,2011. Structural parameters and X-ray Debye temperature determination study on copper ferrite-aluminates, Solid State Sci., 13, 539 – 547,